Atlantis Highlights in Chemistry and Pharmaceutical Sciences, volume 2
Proceedings of the 5th International Conference on Chemical Investigation and Utilization of Natural Resource (ICCIUNR-2021)

Experimental Study on the Effect of Oil Recovery and Transportability Through the Rock Core Using SiO_2 Nanoparticles Fluid for Sandstone

Kazunori Abe[1,*], Taisuke Inomata[1], Shigemi Naganawa[1], Hikari Fujii[1]

[1] *Graduate School of International Resource Sciences, Akita University, Akita, Japan*
[*] *Corresponding author. Email: abe@mine.akita-u.ac.jp*

ABSTRACT
In oil recovery technique using SiO_2 nanoparticles, evaluating the transportability of the nanoparticles in various sandstones contributes to controls of fluid behaviour in petroleum reservoirs and improvement of oil recovery factor. In the core flooding test with high-content kaolinite sandstones, the maximum oil recovery of about 4.5% was obtained by injecting negatively surface charged nanoparticles without adsorption of a large amount of the SiO_2 nanoparticles on the rocks and the pore channels plugging effect. The main mechanisms of the oil recovery were suggested wettability alteration changing to more water-wet on the rock surface and increase of disjoining pressure.

Keywords: *Enhanced oil recovery, Chemical flooding, SiO_2 nanoparticles, Kaolinite, Transportability, Physicochemical interaction*

1. INTRODUCTION

As the demand for crude oil keeps growing and new discoveries of oil reservoirs are declining, enhanced oil recovery (EOR) technique such as gas flooding, thermal flooding, and chemical flooding plays a key role to increase recovery factor for energy demand side [1]. However, large amounts of oil deposits still remain unrecovered after the application of conventional EOR methods such as gas flooding. Chemical EOR has been adjudged as an efficient oil recovery technique to recover bypassed oil and residual oil trapped in the reservoir [2]. Chemical flooding like surfactants is also an important technique to reduce the mobility ratio and to recover the remained oil [3]. However, the injected surfactant solution contacts both reservoir fluid and formation rock surfaces. Therefore, high adsorption of surfactant molecules onto internal pore surfaces in the formation of rock leads to insufficient surfactant molecules to interact with reservoir fluids and makes surfactant flooding economically inapplicable [4, 5]. Recently, applying nanoparticles (NPs) to the EOR technique has been studied. The NPs for EOR techniques such as SiO_2 nanoparticles (SNPs) have been useful materials for oil recovery due to environmentally friendly materials compared to other chemical substances and lower operation costs for water-based fluid without adding other materials and large-scale facilities. Many researchers proposed that (1) disjoining pressure [6, 7], (2) pore channels plugging [8], (3) wettability alteration [9], (4) interfacial tension (IFT) reduction [10] are the main mechanisms of the oil recovery with SNPs. In contrast, the SNPs material in reservoir conditions tend to aggregate each other and adsorb onto a rock surface, which prevents the transport of SNPs in oil reservoirs. In addition, clay minerals in sandstones such as kaolinite have preferentially hydrophobic, or more oil-wet [11-13]. The structure of kaolinite is differently charged sites as surface potential (negatively charged) and edge potential (positively charged) [14]. The surface characteristics of kaolinite minerals may react with SNPs material to occur pore channels plugging. Thus, the relation between clay minerals and the SNPs material in the wettability

alteration process is still required to understand the transportability of the SNPs and oil recovery.

The aim of this research is to elucidate the effects of oil recovery and transportability of SNPs by core flooding test with different kaolinite content in sandstones, which evaluate the relationship with the various factors such as IFT (oil-water), wettability (oil-water-rock), and zeta potential.

2. EXPERIMENTAL

2.1. Materials

The fluid properties used in this experimental study were shown in Table 1. Artificial water, which represents the reservoir formation water, was synthesized of 40000 ppm NaCl using distilled water. The density and viscosity of the artificial water were 1.04 g/cm^3 and 1.01 cP. A 1000 ppm NaCl water was prepared in order to utilize it as primary injection fluid for the flooding test. Negatively charged silica nanoparticles (SNPs-A) and positively charged silica nanoparticles (SNPs-B) were prepared, and both SNPs have a diameter of approximately 12 nm. The silica concentrations of SNPs-A and SNPs-B diluted by 1000 ppm of NaCl water were 1000 ppm. The density and viscosity were 1.04 g/cm^3 and 0.97 cP for SNPs-A and 1.05 g/cm^3 and 0.99 cP for SNPs-B at 20°C. The density and viscosity of crude oil were 0.85 g/cm^3 and 7.7 cP at 20°C.

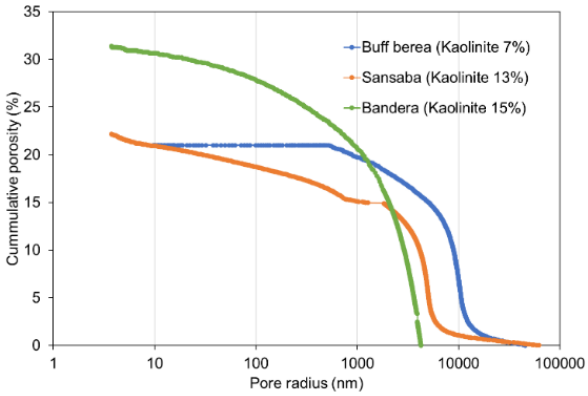

Figure 1. Pore size distributions of the sandstones (Buff Berea, Sansaba, Bandera Brown)

Three areas of sandstone samples are composed of 7%, 13%, 15% kaolinite as shown in Table 2. Pore size distributions (PSDs) and total porosities of the sandstone samples were shown in Figure 1. Buff Berea and Sansaba samples have close porosity of approximately 21-23%, and Sansaba sample has a higher kaolinite content of 13% and narrower pore space than Buff Berea sample. Bandera Brown sample has a high porosity of approximately 31%, which has the almost same kaolinite content and the tendency of PSD as the Sansaba sample.

Table 1. Characteristics of fluid at 20°C

Fluid	Salt concentration (ppm)	SNPs concentration (ppm)	Surface charge	Specific gravity (g/cm^3)	Viscosity (cP)
NaCl	40000	0	-	1.04	1.01
NaCl	1000	0	-	1.01	0.98
SNPs-A	1000	1000	Negative	1.04	0.97
SNPs-B	1000	1000	Positive	1.05	0.99
Crude oil	-	-	-	0.85	7.7

Table 2. Mineral components of the sandstones (Buff Berea, Sansaba, Bandera Brown)

Rock sample	Quartz (%)	Kaolinite (%)	Montmorillonite (%)	Muscovite (%)
Buff Berea	93	7	<0.1	<0.1
Sansaba	86	13	<0.1	<0.1
Bandera Brown	84	15	<0.1	<0.1

2.2. Core Flooding Test

All core plug samples used for the core flooding test were around 25.4 mm in diameter and 50.8 mm in length. The core plugs were cleaned with toluene and methanol to remove organic contaminants, which dried at a temperature of 60°C under a low-pressure condition for more than 24 hours to expel solutions such as water. These core plugs were fully saturated with 40000 ppm NaCl water using a vacuum desiccator. The core plugs were set the core holder of the core flooding apparatus (Vinci Technology, SRP-350) shown in Figure 2, and the samples were saturated with crude oil.

Prior to the core flooding test, the core plugs saturated with crude oil were aged for more than 20 days at 60°C under atmospheric pressure. After these processes, the core plugs were applied to confine pressure of approximately 2000 psi using a hand pump and temperature of 60°C by means of a heat jacket of the core holder. The displacement fluids were injected into core plugs to displace the crude oil in the core flooding test. The procedures of the core flooding test were conducted as following: injecting 1000 ppm NaCl water for primary flooding by the end of oil production (100% water cut), injecting SNPs fluids for secondary flooding by 100% water cut. The core plugs and injection fluids used for the core flooding test were shown in Table 3.

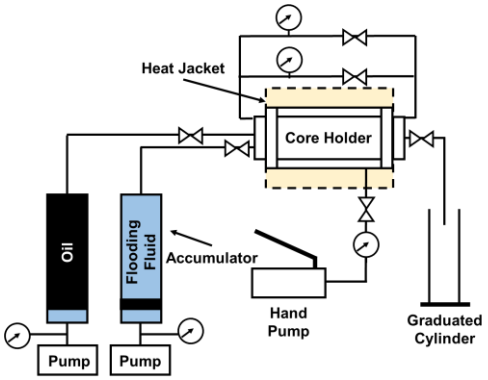

Figure 2. Schematic diagram of core flooding apparatus

Table 3. Core plugs and injection fluids for core flooding test

No.	Rock sample	Diameter (mm)	Length (mm)	Porosity (%)	Water permeability (mD)	Initial oil saturation (%)	Primary injection fluid	Secondary injection fluid
1	**Buff Berea**	25.7	50.7	21.1	110.3	94.7	NaCl 1000 ppm	SNPs-A
2	**Buff Berea**	25.3	50.7	23.3	130.5	81.9	NaCl 1000 ppm	SNPs-B
3	**Sansaba**	25.2	50.5	22.6	41.5	84.3	NaCl 1000 ppm	SNPs-A
4	**Bandera Brown**	24.8	51.1	31.4	50.6	86.5	NaCl 1000 ppm	SNPs-A

2.3. Contact Angle Measurement

Each contact angle between crude oil and rock samples in the SNPs fluids was measured by the rising drop method using a contact angle goniometer (Meiwafosis, Phoenix-300). The contact angle measurements were measured at 20°C under atmospheric pressure.

2.4. IFT Measurement

IFT measurement between crude oil and displacing fluids (SNPs fluids, NaCl water) was determined by the pendant drop method (EKO instrument, OCA35). The IFT measurements were measured at 20°C under atmospheric pressure. The apparatus continuously captured the small oil drop per 10 seconds for 25 minutes.

2.5. Zeta Potential Measurement

The Zeta potential of SNPs and sandstones was measured using the dynamic laser light scattering apparatus (Otsuka Electronics, ELSZ-1000ZS) to evaluate the electrostatic force of the samples.

The interaction between SNPs and sandstones was evaluated by estimating the repulsive and attractive forces of the samples under each pH condition.

2.6. Evaluation of Transportability of the SNPs in Rock Cores

The transportability of the SNPs was firstly evaluated with the amounts of SNPs left in the rock cores after a core flooding test. Then the concentrations of the SNPs in effluent solution through rock cores were estimated by use of microwave plasma atomic emission spectrometer (Agilent Technology, 4210 MP-AES). The concentration of SiO_2 was calculated based on the standard curve of Si (standard solution: 1 ppm, 5 ppm, 10 ppm). For fitting the range of the standard curve, 100 times diluted effluent solutions were prepared. The effluent solutions through rock cores were collected each 1 Injected Pore Volume (PV) in core flooding tests.

To evaluate the plugging effects of SNPs, the gas permeability of the rock core after the core flooding test was measured. After the core flooding test, the core plugs were kept in toluene and methanol for removing crude oil and salt components in the cores for 7 days. After the cleaned cores were dried, the permeability of each core plug was measured, and compared with the initial gas permeability. The gas permeability of the cores was measured using a gas porosimeter (Vinci Technology, Poro Perm).

3. RESULT AND DISCUSSION

3.1. Core Flooding Test

The core flooding tests were carried out to measure oil recovery factor and differential pressure by injecting 1000 ppm NaCl water and 1000 ppm SNPs fluids. In the case of Buff Berea (kaolinite 7%), Figure 3 shows that oil recovery for (a) SNPs-A (negatively surface charged) fluid flooding and (b) SNPs-B (positively surface charged) fluid flooding was obtained 4.1% and 2.0%, respectively. The differential pressure behaviour showed an almost steady in the injection process of SNPs-A, while the increases of differential pressure could be observed in the injection process of SNPs-B. Since the SNPs-B and the rock sample have different surface charges, positive and negative, a large amount of SNPs were adsorbed on the rock surface, causing pore channels plugging effect.

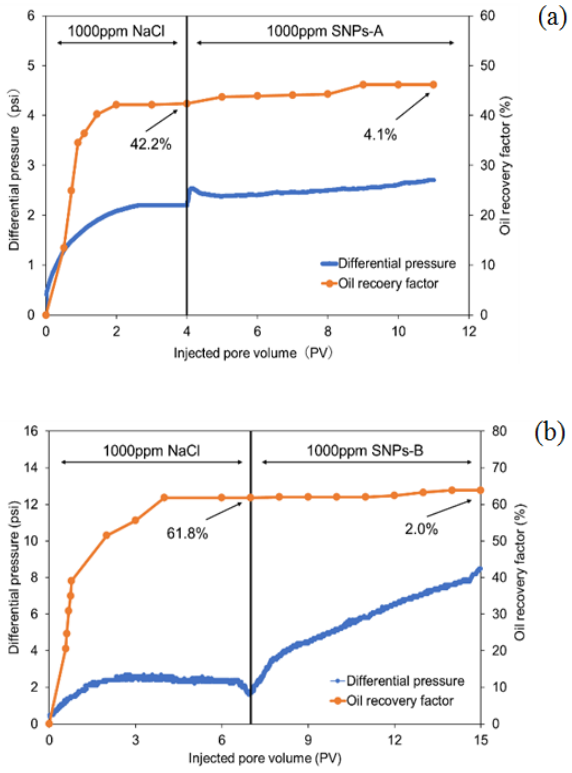

Figure 3. Oil recovery factor and differential pressure in the core flooding test for Buff Berea with (a) SNPs-A, (b) SNPs-B

Figure 4 shows that oil recovery for (a) Sansaba (kaolinite 13%) and (b) Bandera Brown (kaolinite 15%) was obtained 4.4% and 4.5% by injecting SNPs-A, respectively. The Sansaba showed a relatively high pressure due to its lower total porosity than Bandera Brown with the same trend of micro-pores. In addition, the pressure increase in the SNPs injection process in Figure 4 (a) was due to the slight plugging effect caused by the pore characteristics of Sansaba.

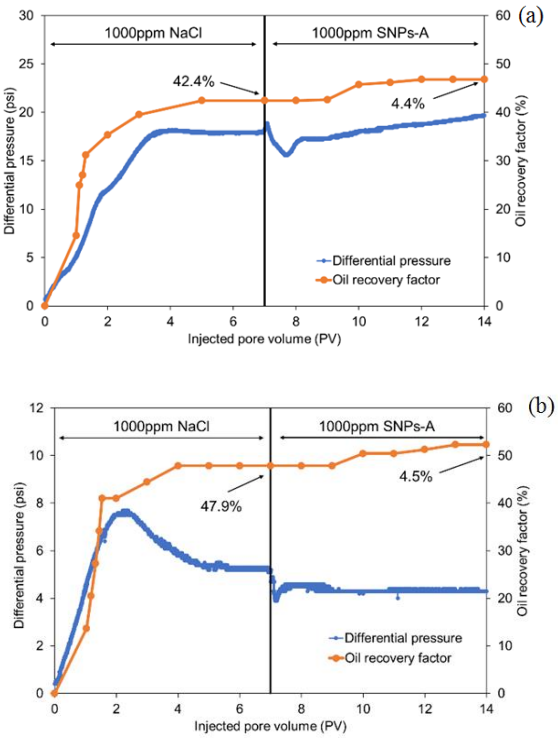

Figure 4. Oil recovery factor and differential pressure in the core flooding test with SNPs-A for (a) Sansaba, (b) Bandera Brown

3.2. Contact Angle Measurement

The contact angle in a three phases system is defined as water-wet in the range of 105° to 180°, intermediate-wet in the range of 75° to 105°, and oil-wet in the range of 0° to 75° for this experiment. The measurement of the contact angle between crude oil and rock in the SNPs fluids or salinity water at 20°C under atmospheric pressure is shown in Figure 5. The contact angle with SNPs-A and SNPs-B fluids for Buff Berea was increased from 141.8° to 147.8° and 140.6° to 145.4°, respectively (Figure 5 (a)). Both SNPs-A and SNPs-B could change the wettability of the rock to more water-wet compared with only NaCl water. On the other hand, the contact angle with SNPs-A fluids for Buff Berea (kaolinite 7%), Sansaba (kaolinite 13%), and Bandera Brown (kaolinite 15%) increased from 141.8° to 147.8°, 140.5° to 150.6° and 143.6° to 148.2°, respectively. These results suggest the improvement of the

displacement efficiency based on the wettability alteration changing to more water-wet.

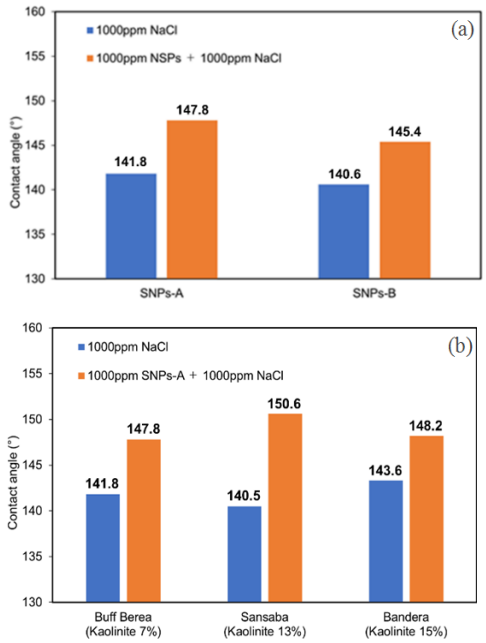

Figure 5. Contact angle results (a) SNPs-A and SNPs-B for Buff Berea, (b) SNPs-A for Buff Berea, Sansaba and Bandera Brown at 20°C

3.3. IFT Measurement

The pendant drop method was used in this experiment to quantify the IFT value between crude oil and 1000 ppm SNPs-A fluid, 1000 ppm NaCl.

IFT was measured to evaluate displacement efficiency between fluid and fluid by capillary number (N_c), which is determined Equation (1).

$$N_c = \frac{\mu \times v}{\sigma} \quad (1)$$

Where μ is viscosity (cP), v is darcy's velocity (m/s), σ is interfacial tension (mN/m). If the capillary number is under 10^{-5}, oil trapped in the reservoir may generally start to move [15].

Table 4. The values of a parameter of fluid at 20°C and the capillary number

Sample	Viscosity (cP)	Interfacial tension (mN/m)	Darcy's velocity (m/s)	Capillary number
1000 ppm NaCl	0.98	1.82	6.63×10^{-6}	3.57×10^{-6}
1000 ppm SNPs-A	0.97	2.22	6.63×10^{-6}	2.90×10^{-6}

Figure 6 shows that the IFT between 1000 ppm NaCl and crude oil is about 1.82 mN/m, and the IFT between 1000 ppm SNPs-A fluid and crude oil is about 2.22 mN/m. According to the calculating value of the capillary number applied by the IFT values, it indicated that SNPs-A would hardly affect the improvement of the displacement efficiency for the crude oil used in this experiment (Table 4).

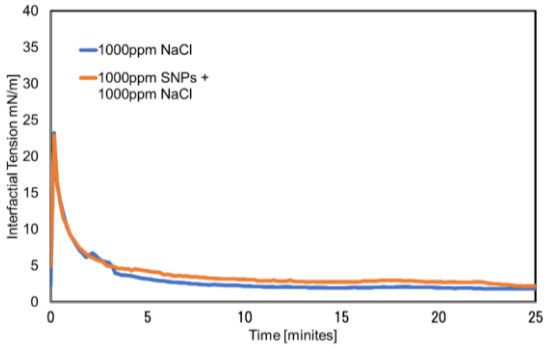

Figure 6. IFT between crude oil and 1000 ppm SNPs-A fluid, 1000 ppm NaCl at 20°C

3.4. Zeta-Potential Measurement

Figure 7 shows that the zeta potentials of Buff Berea (kaolinite 7%), Sansaba (kaolinite 13%), and Bandera Brown (kaolinite 15%) have negative values due to the negatively charged quartz in the sandstone samples. The absolute value of the zeta potential of Bandera Brown (kaolinite 15%) tended to be lower than Buff Berea (kaolinite 7%) due to the interaction of positively charged kaolinite. The grey colour area in Figure 7 demonstrates the pH conditions in the core flooding test. SNPs-B has positive charges under the pH conditions, suggesting that a surface electric charge is one of the factors of the pugging effect.

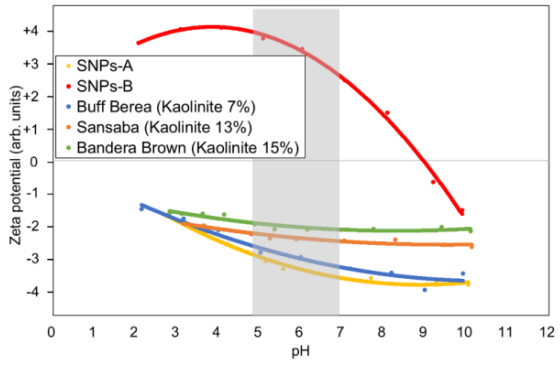

Figure 7. Zeta potential for the sandstone samples and SNPs depending on pH

3.5. Evaluation of transportability of the SNPs in rock cores

SNPs concentration in the effluent in the core flooding test was measured to estimate the amounts of SNPs left in the core (Figure 8). In Figure 8, the fluid injection processes are divided into three parts; section (A) is 1000 ppm NaCl water as primary flooding, section (B) is 1000 ppm SNPs fluid as secondary flooding, and section (C) is 1000 ppm NaCl water as post flush. The red dash line in Figure 8 demonstrates the concentration of the injection of SNPs in the core flooding tests. In Figure 8 (a), the SNPs-A concentration in effluent reached the peak (red dashed line) in the section (B). In the post flush process of section (C), its concentration was decreased to almost the same level in section (A), which indicated the SNPs-A left in the core were removed by the post flush, while most of SNPs-B were left in the cores based on the SNPs-B concentration in section (B) and (C). In this core flooding test of Figure 8 (a), 8.4% of SNPs-A was left in the Buff Berea (kaolinite 7%) with respect to the amount of SNPs-A injection, while 95% of SNPs-B was left in the rock core. In the case of different rock types of Figure 8 (b), SNP-A reached the peak and most of SNPs-A were discharged in the post-flush processes.

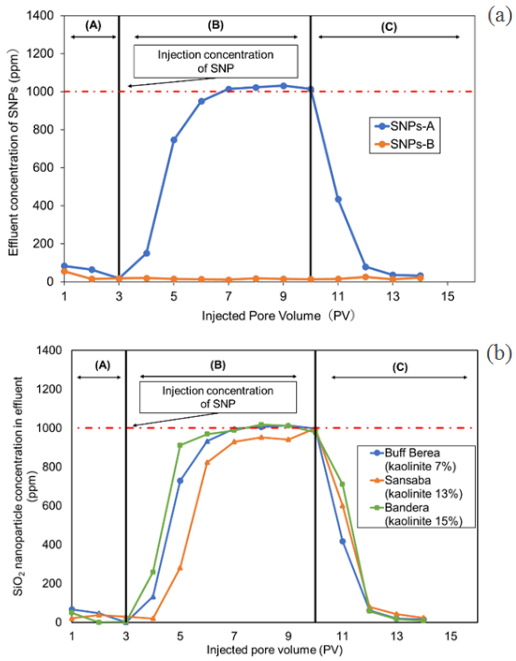

Figure 8. SNPs concentration in the effluent in the core flooding tests (a) with SNPs-A and SNPs-B for Buff Berea, (b) with SNPs-A for Buff Berea, Sansaba and Bandera Brown

The amount of SNPs-A left in the Sansaba (kaolinite 13%) and the Bandera Brown (kaolinite 15%) was estimated to be 18.6% and 5.7%, respectively. Sansaba sample, which has high kaolinite contents and low permeability, had relatively more SNPs-A left in the core than other rock samples.

Table 5 shows the reduction ratio of gas permeability of the rock cores before and after the core flooding test. In the case of SNPs-B, the reduction rate of gas permeability was 63.3%, while the reduction rate of SNPs-A with the same rock sample (Buff Berea) was 7.7%. It suggests that the pore plugging effect of SNPs-B was remarkable. The reduction rates of the permeability correlate with the SNPs concentration in the effluent (Figure 8), which supports the understanding of the transportability of SNPs in the rock cores.

Table 5. The change of gas permeability of core plugs after SNPs flooding

Injection fluid in core flooding test	Rock sample	Gas permeability (mD)		Reduction ratio of gas permeability (%)
		Before SNPs flooding	After SNPs flooding	
SNPs-B 1000 ppm	Buff Berea	361.3	230.3	63.3
SNPs-A 1000 ppm	Buff Berea	316.2	291.9	7.7
	Sansaba	68.2	54.5	20.1
	Bandera Brown	74.2	69.8	5.9

3.6. Evaluation of total energy of interaction

The oil recovery effect and transportability of SNPs in this experiment are discussed from the perspective of the total energy of interaction in this section. At first, evaluation of the interaction between SNPs and rock surface was conducted by use of the Derjaguin - Landau - Verwey - Overbeek (DLVO) theory. This theory shows that when two particles are near each other, the stability of particles in solution is affected by the total energy of interaction (V_T), which is determined by Equation (2).

$$V_T = V_{DLR} + V_{LVA} \quad (2)$$

where V_{DLR} is the electric double-layer energy and V_{LVA} is the attractive energy. V_{DLR} is expressed as Equation (3) [16].

$$V_{DLR} = (\varepsilon A_p/4)\left\{2\zeta_1\zeta_2 \ln\left[\frac{1+\exp(-\kappa h)}{1-\exp(-\kappa h)}\right] + (\zeta_1^2+\zeta_2^2)\ln[1-\exp(-2\kappa h)]\right\} \quad (3)$$

where V_{DLR} is the electric double-layer energy. ζ is zeta potential of the sample, ε is dielectric constant, A_p is the size of SNPs, h is the distance of the two particles, and κ is Debye length. To estimate $V_{DLR,}$ the zeta potential (ζ_1 and ζ_2) measured in the previous section is applied to the equation. The positive sign shows that this energy is repulsive dominantly. Equation (4) is presented for V_{LVA} [16].

$$V_{LVA} = \frac{-A_H}{6} \times \left[\frac{2\times(1+H)}{H\times(2+H)} + \ln\left(\frac{H}{2+H}\right)\right] \quad (4)$$

V_{LVA} is the London-van der Waals energy and plays an important role in reinforcing the attachment of particles to pore surfaces. The negative sign shows this energy is attractive dominantly. Where A_H is the Hamaker constant, H is the distance of separation. To prevent the concealment of dimensions in the calculation, the dimensionless form of the V_T is obtained from V_T divided by the product of the Boltzmann constant K_B and temperature T. Equation (5) shows the dimensionless form of this total energy.

$$V_{TD} = \frac{V_T}{K_B \times T} \quad (5)$$

where V_{TD} is the dimensionless form of the total energy of interactions. Table 6 shows the values for calculating V_{TD}. Debye length referred to the reference [16].

Since the effluents in the core flooding test had a pH of around 6.8, the V_{TD} between SNPs and the rock surface was calculated by use of the zeta potential at the point. The calculated V_{TD} focused on both SNPs with Buff Berea (kaolinite 7%) is shown in Figure 9 (a). As the results, when the distance of SNPs-A and Buff Berea surface is close, SNPs-A has repulsive due to the positive value of V_{TD}, while SNPs-B has attractive due to the negative values of V_{TD}. The calculated V_{TD} between SNPs-A and Buff Berea (kaolinite 7%), Sansaba (kaolinite 13%), and Bandera Brown (kaolinite 15%) were negative values, as shown in Figure 9 (b). SNPs-A has stable adsorption on the rocks and dispersion in the sandstone cores regardless of the kaolinite contents.

3.7. The mechanism of oil recovery with SNPs

Disjoining pressure is considered as one of the mechanisms of oil recovery with SNPs. Disjoining pressure is presented by Equation (6) [17].

$$\Pi = \Pi_{vw} + \Pi_d + \Pi_{st} \quad (6)$$

where Π is the disjoining pressure, Π_{vw} is the van der Waals force, Π_d is electrostatic and Π_{st} is the structural forces arising from the ordering of the nanofluid's particles in the wedge film. Based on the calculations of the total energy of interaction between SNPs-A and Buff Berea, Sansaba, and Bandera Brown, the electrostatic Π_d works to maintain the repulsion force, which forms the disjoining pressure.

Table 6. Constant values for the calculation of V_{TD}

Constant	Value
Dielectric constant (ε)	8.9×10^{-12}
Particle radius (A_p)	12×10^{-9}m
Debye length (κ)[16]	$(9.6\times10^{-9})^{-1}$ m
Hamaker constant (A_H)	6.0×10^{-21} J
Boltzmann constant (K_B)	1.4×10^{-23} J/K
Temperature (T)	333 K

This is the reason the contact angle between SNPs-A and each rock sample could be changed to more water-wet (Figure 9 (b)). Also, the total energy of interaction between SNPs-B and Buff Berea might be shown that the rock surface was modified to be more water-wet due to the adsorption of the SNPs-B on the rock surface (Figure 9 (a)).

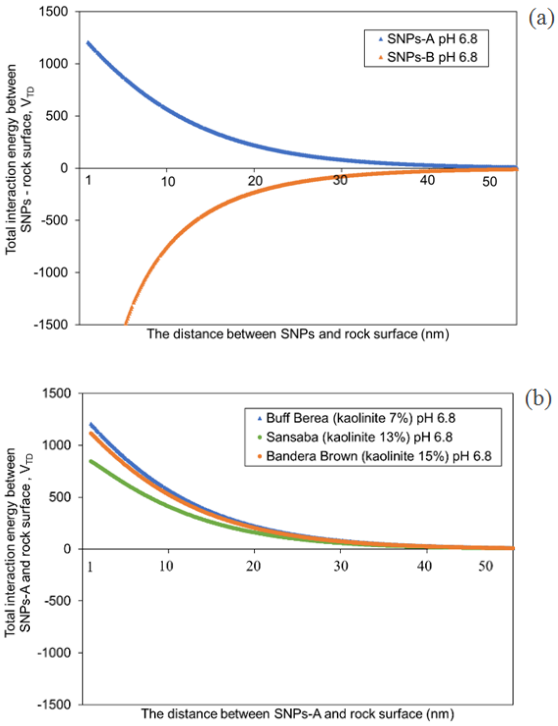

Figure 9. The calculated V_{TD} is the distance of SNPs and rock surface: (a) V_{TD} between SNPs-A, SNPs-B, and Buff Berea, (b) V_{TD} between SNPs-A and Buff Berea, Sansaba and Bandera Brown

4. CONCLUSION

In the core flooding test with negatively charged SNPs-A, the maximum oil recovery factor of about

4.5% was obtained even with high-content kaolinite sandstones. The main mechanism of the oil recovery was wettability alteration changing to more water-wet on the rock surface in this experiment conditions, which works disjoining pressure between crude oil, SNPs fluid, and rock. The positively surface charged SNPs-B was highly adsorbed on the rock surface, causing pore channels plugging effect. In contrast, it was suggested that the transportability of SNPs-A is effective for various sandstones.

ACKNOWLEDGMENT

This research was supported by JSPS KAKENHI Grant Number JP21K04959 and Akita University Support for Fostering Research Project.

REFERENCES

[1] Alvado V., Manrique E., (2010) Enhanced oil recovery: an update review. Energies, Vol. 3(9), 1529-1575.

[2] Gbadamosi A.O., Iunin R., Manan M.A., Agi A., Yusuff A.S., (2019) An overview of chemical enhanced oil recovery: recent advances and prospects. International Nano Letters, 171-201.

[3] Sandersen S.B., (2012) Enhanced Oil Recovery with Surfactant flooding, Ph.D thesis, Technical University of Denmark, Sci. Eng, 736022015.

[4] Ngo I., Srisuriyachai F., Sugai Y., Sasaki K., (2017) Study of Heterogeneous Reservoir Effects on Surfactant Flooding in Consideration of Surfactant Adsorption Reversibility, the SPWLA 23rd Formation Evaluation Symposium of Japan, SPWLA-JFES-2017-A.

[5] Vargo J., Turner J.,Vergnani B., Pitts M.J., Wyatt K., Surkalo H., Patterson D., (2000) Alkaline-surfactant-polymer flooding of the Cambridge Minnelusa field. SPE Reservoir Evaluation and Engineering. Vol. 3, 552–558.

[6] Mcelfresh P.M., Olguin C., Ector D., (2012) The application of nanoparticle dispersions to remove paraffin and polymer filter cake damage. In Proceedings of the SPE International Symposium and Exhibition on Formation Damage Control, Lafayette, LA, USA, 15–17.

[7] Aveyard R., Binks B.P., Clint J.H., (2003) Emulsions stabilized solely by colloidal particles. Advences In Colloid and Interface Science, Vol. 100, 503–546.

[8] Skauge T., Spildo K., Skauge A., (2010) Nano-Sized particles for EOR. The SPE Improved Oil Recovery Symposium, Tulsa, OK, USA, 24–28.

[9] Giraldo J., Benjumea P., Lopera S., Cortes F.B., Ruiz M.A., (2013) Wettability alteration of sandstone cores by alumina-based nanofluids. Energy Fuels, Vol. 27, 3659-3665.

[10] Hendraningrat L., Li S., Torsaeter O.A., (2013) Coreflood investigation of nanofluid enhanced oil recovery. Journal of Petroleum Science and Engineering, Vol. 111, 128–138.

[11] Awolayo A.N., Sarma H.K., Nghiem L.X., (2018) Brine-Dependent Recovery Processes in Carbonate and Sandstone Petroleum Reservoirs. Review of Laboratory-Field Studies, Interfacial Mechanisms and Modelling Attempts. Energies, 11, DOI: 3020. 10.3390/en11113020.

[12] Borysenko A., Clennell B., Sedev S., Burgar I., Ralston J., Raven M., Dewhurst D., Liu K., (2009) Experimental investigations of the wettability of clays and shales. Journal of Geophysical Research, Vol. 114(B7), DOI:10.1029/2008JB005928

[13] Bantignies J.L., Moulin C.C.D., Dexpert H., (1997) Wettability contrasts in kaolinite and illite clays: Characterization by Infrared and X-ray Absorption Spectroscopies. Journal de Physique IV Proceedings, EDP Sciences, Vol. 7(C2), 867-869.

[14] Elimelech M., O'Melia C.R., (1990) Kinetics of deposition of colloidal particles in porousmedia. Environmental Science and Technology, Vol. 24(10), 1528-1536. DOI: 10.1021/es00080a012

[15] Guo H., Dou M., Hanqing W., Wang F., Yuanyuan G., Yu Z., Yansheng W., Li Y., (2017) Proper use of capillary number in chemical flooding. Hindawi Journal of Chemistry, 1-11, DOI: 10.1155/2017/4307368

[16] Khilar K.C., Fogler H.S., (1998) Colloidally Induced Release of Fines in Porous Media Migration of Fine in porous media. Springer, Dordrecht, 29-61.

[17] Wasan D., Nikolov A., Kondiparty K., (2011) The wetting and spreading of nanofluids on solids: Role of the structural disjoining pressure. Current Opinion in Colloid & Interface Science, Vol. 16, 344-349.